# Dynamic Modeling and Multivariable Model Predictive Control of the Air Separation Columns in an IGCC Power Plant

Tongshu Guo, Jianhong Lu, Wenguo Xiang, Weiming Ding and Tiejun Zhang

***Abstract*—Integrated Gasification Combined Cycle (IGCC) is one of the most promising and competitive energy producing and coal utilization technologies. A typical IGCC plant mainly consists of an air separation unit, gasification system, gas turbine, heat recovering boiler and a steam turbine. This paper investigates the characteristics of the cryogenic rectification column, which is the core of the air separation unit. It will strongly affect the overall system's transient behavior. A control-oriented first-principle mathematic model is developed for the double column, and the dynamic characteristics are presented. Furthermore, in order to optimize the transient operation performance of the air separation unit, a multivariable predictive control strategy for the column is presented and discussed.**

***Index Terms*—Air separation units, dynamic modeling, IGCC, Multivariable model predictive control**

## I. Introduction

With the development of the society, the demand for power and electricity is increasing at an alarming rate worldwide. Unfortunately, the energy industry today is facing serious problems and challenges, such as the limited natural resources, the global warming, the appearance of acid rain and the degradation of ecological [1]. To solve these problems, it is expected that the electricity producing methods will be altered by the efficiency and environmental regulations factors in the near future [2].

An Integrated Gasification Combined Cycle (IGCC) power plant, including coal gasification process, air separation unit, and the combined-cycle unit, is one of the key solutions to meet the requirements. It has a lot of advantages over conventional solid fuel combustion power plants, mainly including reduced plant size, higher thermal efficiency and much less emissions, fuels and products flexibility. All of them make it by far the best concept for electricity and thermal energy generation [3], [4]. The air separation unit (ASU) has been developed for many decades and successfully used to supply oxygen for the gasification in IGCC power plants [5], [6], [7]. The cryogenic air separation unit operates at extremely low temperatures of about 100 K, which is in fact a distillation process for the generation of high purity nitrogen, oxygen and argon from air according to their different boiling temperatures. This kind of ASU generates oxygen at the concentration of about 95% for coal gasification, consumes about 10% of the gross power output, and requires about 15% of the total plant cost. Moreover, the ASU is usually the slowest component in an IGCC plant, and its dynamic response affects the behaviors of the plant greatly. With it optimally integrated with the gas turbine, the net cost of power generation can be decreased while the efficiency increased [8], [9]. Therefore, it is desirable to investigate the advanced regulatory control strategy for the air separation unit, so as to optimize its transient operations and eventually to improve the overall energy efficiency.

The paper is organized as follows: firstly, a brief description is given to introduce the flow diagram of the air separation unit and its connection with the gas turbine. Secondly, under some reasonable assumptions, a first principles "stage-by-stage" model for the column is developed in forms of differential and algebraic equations. Thirdly, the dynamic characteristics of the double column are discussed with several mass flows step changes introduced. Finally, a control structure for the column is presented and the performance of the controllers is simulated and discussed.

## II. Process Description

As shown in Fig. 1, the cryogenic air separation unit in IGCC plant is comprised of the high pressure (HP) column, low pressure (LP) column, the main heat exchanger, and a condenser-reboiler system providing internal thermal coupling effect. Compressed air from the combined-cycle island is led through an absorber to remove water, carbon dioxide and some other impurities avoiding ice formulation in the downstream equipment [8], [10]. A small portion of the feed stream is used as "expand air" compensating the column heat losing to the environment and introduced to stage 24 of LP column [8]. The rest is cooled in the main heat exchanger and flows to the bottom of HP column as main feed of the ASU. In the HP column, high purity nitrogen is obtained at the top and oxygen-rich liquid air is collected at the bottom.

Manuscript received July 3, 2009. This work was supported by the National High Technology Research and Development of China (2006AA05A107).

Tongshu Guo is with the Department of Energy Information and Automation, School of Energy and Environment, Southeast University, Nanjing, P.R. China, (phone: +86-13851852528; e-mail: guotongshu@gmail.com).

Jianhong Lu is with the Department of Energy Information and Automation, School of Energy and Environment, Southeast University, Nanjing, P.R. China, (e-mail: jhlv@seu.edu.cn).

Wenguo Xiang is with the Department of Thermal Engineering, School of Energy and Environment, Southeast University, Nanjing, P.R. China, (e-mail: wgxiang@seu.edu.cn).

Weiming Ding is with the Department of Energy Information and Automation, School of Energy and Environment, Southeast University, Nanjing, P.R. China, (e-mail: wmding@seu.edu.cn).

Tiejun Zhang is with the Center for Automation Technologies and Systems, Rensselaer Polytechnic Institute, NY, USA, (e-mail: tjzhang@ieee.org).

The high purity gaseous nitrogen at the top of the HP column is divided into two parts, the first part is drawn out and usually used for the transport of pulverized coal and for various purge flows of the equipment, the second is delivered to the condenser and cooled to be liquid form. One part of the liquid nitrogen flows down as the reflux stream of the HP column, the other is pumped to the top of the LP column and used as reflux stream of the rectifying section [11], [12], [13].

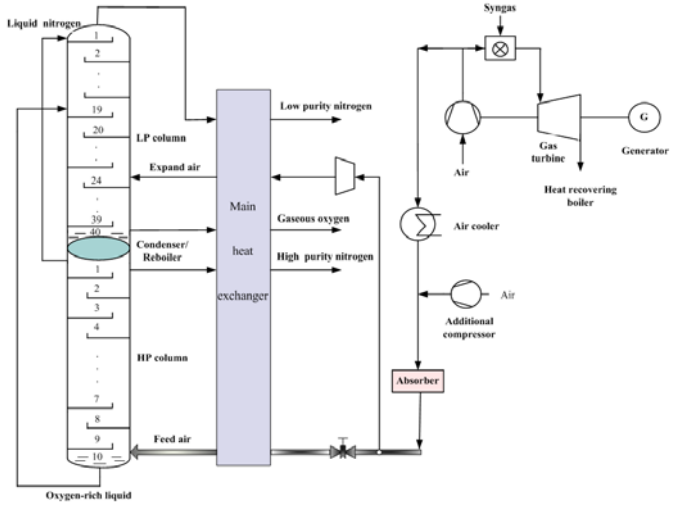


Fig.1. Schematic diagram of the air separation unit process and the air-side connection with the gas turbine.

## III. Model of the Double Column

As stated above, the complete model consists of the model of the column stages and the condenser-reboiler system.

### A. Model of the Theoretical Stage

The model for each tray is generally comprised of differential equations for the total and components mass balances and energy balances, and a set of algebraic equations for vapor-liquid phase equilibrium relations and fraction summation equations (MESH equations). In this paper the model derivation was based on the following reasonable simplifying assumptions [2], [10], [14]:

- the liquid and vapor are ideally mixed respectively on each stage, and the pressure and temperature on a tray are uniform;
- vapor-liquid equilibrium is assumed to be ideal;
- linear pressure drop in each column;
- weeping and entrainment are ignored;
- supposing air as a ternary mixture of nitrogen (78.1%), oxygen (20.95%) and argon (0.95%).

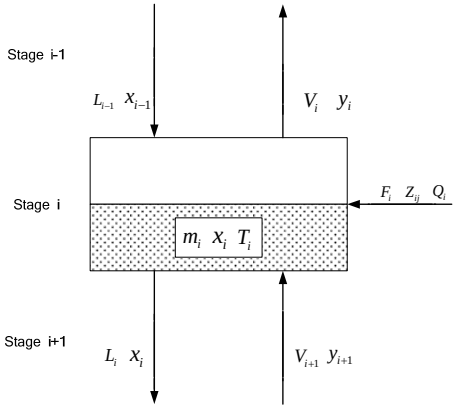


Fig.2. Schematic diagram of a theoretical stage.

The MESH equations for a theoretical stage i (see Fig. 2) can be formulated as followings.

The total material balance (M equation) is given by:

$$\frac{dm_i}{dt} = L_{i-1} - L_i + V_{i+1} - V_i + F_i \tag{1}$$

where $m_i$ is the liquid hold-up of stage i, L the liquid flow, V the vapor flow, and F the feed flow.

The components mass balances of nitrogen and oxygen:

$$m_i \frac{dx_{i,N_2}}{dt} = L_{i-1}x_{i-1,N_2} - L_i x_{i,N_2} + V_{i+1}y_{i+1,N_2} - V_i y_{i,N_2} + F_i z_{i,N_2} - x_{i,N_2}\frac{dm_i}{dt} \tag{2}$$

$$m_i \frac{dx_{i,O_2}}{dt} = L_{i-1}x_{i-1,O_2} - L_i x_{i,O_2} + V_{i+1}y_{i+1,O_2} - V_i y_{i,O_2} + F_i z_{i,O_2} - x_{i,O_2}\frac{dm_i}{dt}$$

where $x$ is liquid phase concentration of the corresponding subscript component, y the vapor phase concentration, and z the feed flow concentration.

The vapor-liquid phase equilibrium relations of nitrogen and oxygen (E equations) are written as [14], [16]:

$$y_{i,N_2} = \frac{\alpha_{N_2} x_{i,N_2}}{1 + (\alpha_{N_2} - 1)x_{i,N_2} + (\alpha_{O_2} - 1)x_{i,O_2}} \tag{3}$$

$$y_{i,O_2} = \frac{\alpha_{O_2} x_{i,O_2}}{1 + (\alpha_{N_2} - 1)x_{i,N_2} + (\alpha_{O_2} - 1)x_{i,O_2}}$$

where $\alpha$ is the relative volatility of the composition, and assumed to be constant in this study.

The fraction summation equations (S equations) are:

$$1 = x_{i,N_2} + x_{i,O_2} + x_{i,Ar}$$
$$1 = y_{i,N_2} + y_{i,O_2} + y_{i,Ar} \tag{4}$$

The heat balance equations (H equations) are:

$$m_i \frac{du_i}{dt} = L_{i-1}h^L{}_{i-1} + V_{i+1}h^V{}_{i+1} - L_i h^L{}_i - V_i h^V{}_i + F_i h^F{}_i + Q_i - u_i \frac{dm_i}{dt} \tag{5}$$

where u is the internal energy of the unit-mass liquid phase, h the enthalpy, and Q the heat flow.

### B. Hydraulic Model and Physical Properties

Variables defined by thermodynamic relations such as pressure, temperature, liquid flow are needed to complete the model.

In the present paper, the liquid hydraulics is considered by including a linear Francis Weir formula and liquid flow from the tray is [17], [18]:

$$L_i = L_i^0 + \frac{m_i - m_i^0}{\tau_i} \tag{6}$$

where $L_i$ and $L_i^0$ are the current and initial value of the liquid flow rate of stage i, $m_i$ and $m_i^0$ the current and initial holdups, respectively, and $\tau_i$ the tray hydraulic time constant can be calculated by:

$$\tau_i = \frac{m_i^0}{2L_i^0} \tag{7}$$

Besides, we assume constant liquid and vapor mass flow along the column [16], that is, if there is no feed flow to the column or products removal from the stages, at steady-state:

$$L_i = L_{i+1};\ V_i = V_{i+1} \tag{8}$$

When there is a feed flow to stage i or the feed flow changes, the liquid and vapor flow can be formulated:

$$L_i' = L_i + q_F F_i;\ V_i' = V_i + (1 - q_F)F_i \tag{9}$$

where $F_i$ is feed flow to stage i, $q_F$ the liquid fraction in the feed flow, and $L_i'$ and $V_i'$ are the resulted liquid and vapor flow, respectively.

A linear increase of the stage pressure from a constant overhead pressure $P_1$ was assumed:

$$P_i = P_1 + (i-1)\Delta P \tag{10}$$

A constant stage pressure drop was correlated to the reboiler vapor rate ($V_r$) using Aspen simulation data:

$$\Delta P = \beta V_r^2 \tag{11}$$

where $\beta$ is a constant [10].

As for temperature of the saturated mixture, it can be determined from concentrations and pressure according to Raoult's law, with a polynomial approximation of temperature as a function of nitrogen saturation pressure:

$$p_s = \frac{y}{x} p \tag{12}$$

$$T_s = -1.362e-3\,p_s^4 + 5.490e-2\,p_s^3 - 8.558e-1\,p_s^2 + 7.6778\,p_s + 71.1295 \tag{13}$$

where $p$ has dimension [bar], and $T_s$ [K] [10].

### C. Model of the Condenser-Reboiler System

As shown in Fig.1, the HP column and LP column are thermally coupled by the condenser-reboiler system, as shown in a simplified illustration in Fig. 3. To model the condenser-reboiler system, the following two assumptions are invoked [7], [14]:

- the vapor flow to the condenser will be totally condensed and all the heat released will be used in the reboiler;
- the reboiler and condenser behave like a normal tray, except the calculation of the heat flow from the condenser to the reboiler,

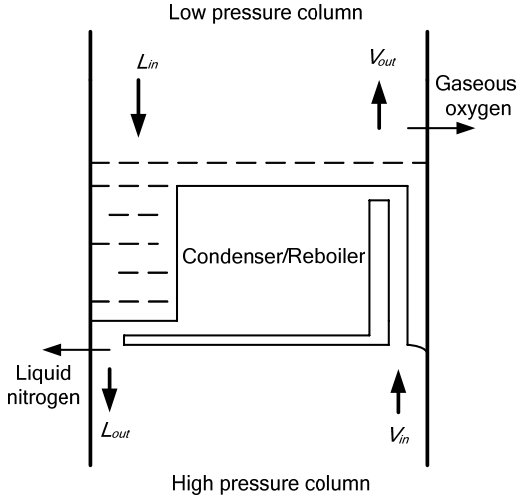


Fig.3. Combined condenser-reboiler system.

The first part of the condenser-reboiler system modeling is to treat the condenser and reboiler the same as a normal tray, and the equations are omitted here preventing repetition. Secondly, the heat flow $Q$ can be calculated with:

$$Q = k \cdot A(T_{head}^{HP} - T_{bottom}^{LP}) \tag{14}$$

where $k \cdot A$ is the overall heat transfer coefficient, $T_{head}^{HP}$ is the temperature at the top of HP column and $T_{bottom}^{LP}$ the temperature at the bottom of LP column. A simple empirical equation for the calculation of heat transfer coefficient is [7]:

$$k \cdot A = c \cdot V_{in}^{0.8} \tag{15}$$

## IV. Dynamic Simulation Study

In order to display the dynamic characteristics of the column, the feed air mass flow, the liquid nitrogen mass flow, and the product nitrogen and oxygen mass flows (see Fig.1) will be introduced to step changes, respectively. And the differential and algebraic equations are implemented in MATLAB/Simulink based simulation environment and are numerically solved with the MATLAB-Solver ode45.

### A. A Step Change of Feed Air Mass Flow

In this subsection a step change of feed air mass flow from 74 kg/s to 78 kg/s is introduced. Fig.4 shows dynamic responses of liquid and vapor flow in HP column and Fig.5 shows the dynamic responses of liquid weight fractions of nitrogen and oxygen in both columns. In the figure, (a) and (b) represent the liquid nitrogen and oxygen weight fractions at the top and bottom of HP column, respectively, (c) and (d) denote the nitrogen and oxygen liquid weight fractions at the top and bottom of LP column. And (a), (b), (c) and (d) in Figure 8, 9 and 10 have the same meaning. From the four plots it can be concluded that oxygen weight fractions in both columns are obviously influenced by the feed air flow, whereas the nitrogen weight fractions are minor influenced.

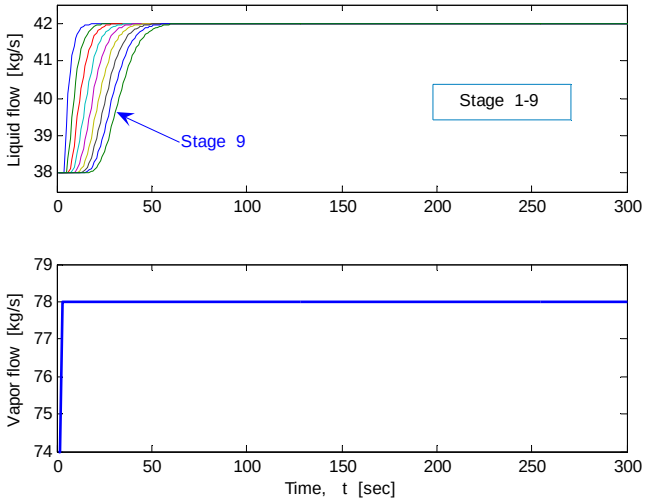


Fig.4. Steady-state profiles of liquid weight fractions of nitrogen, oxygen and argon in LP column.

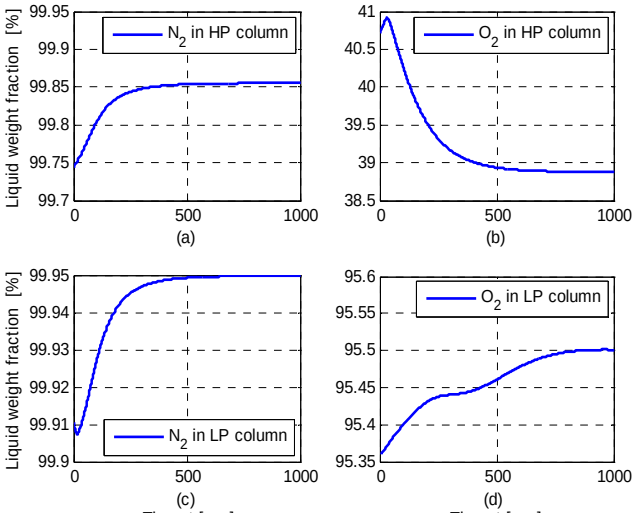


Fig.5. Dynamic responses of liquid weight fractions to a step change of feed air mass flow.

### B. A Step Change of Liquid Nitrogen Mass Flow

In this part a step increase of liquid nitrogen mass flow from 30 kg/s to 33 kg/s is imposed. Fig.6 shows the liquid dynamics in LP column, and liquid flow increases in all stages from the top of the column downward. Fig.7 illustrates the dynamic responses of nitrogen and oxygen weight fractions. When liquid nitrogen mass flow increases, reflux flow of the rectifying section in LP column increases (L/V-ratio increases) while that of the HP column decreases [2]. As a result, in the HP column the nitrogen weight fraction at the top decreases while the oxygen weight fraction at the bottom increases, as shown by plots (a) and (b). From plot (d) we know the oxygen weight fraction in LP column decreases acutely. Within the simulation time of 2000 seconds, still the oxygen fraction has not become steady, which can be a proof that the concentration dynamics is a long-term process.

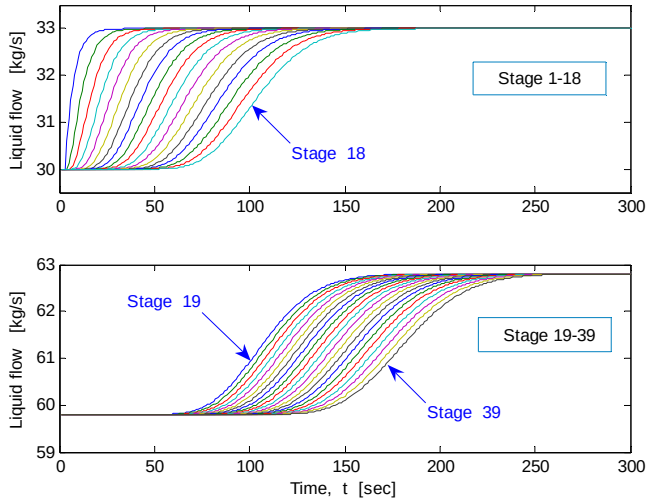


Fig.6. Responses of liquid flow in LP column to a step increase of liquid nitrogen mass flow.

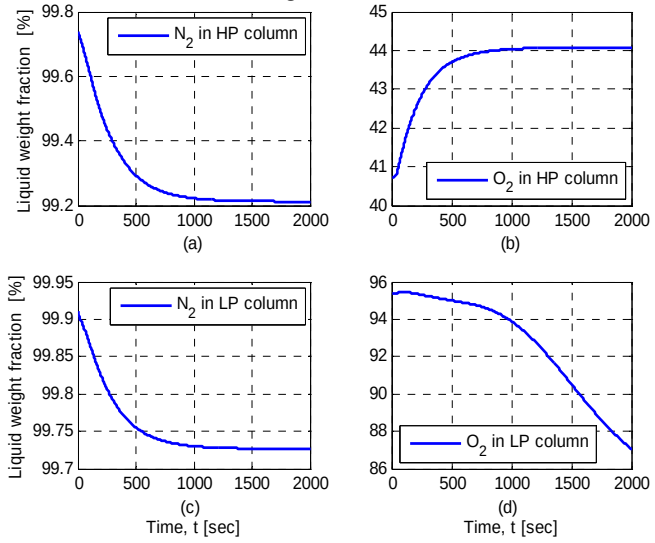


Fig.7. Dynamic responses of liquid weight fractions to a step change of liquid nitrogen mass flow.

### C. A Step Change of Product Nitrogen Mass Flow

Fig.8 shows the dynamic responses of nitrogen and oxygen weight fractions to an increase of low purity product nitrogen mass flow from 56.4 kg/s to 60 kg/s. Because the low purity nitrogen is a product from LP column, and there is no material or heat flow from LP column to HP column, the HP column is little affected, as proved by plots (a) and (b). That is liquid nitrogen and oxygen weight fractions in HP column almost keep constant. Besides, from the figure we can see that with the nitrogen mass flow increases, the nitrogen concentration decreases distinctly. As a result, in order to maintain the nitrogen fraction at a constant level, sharp changes of the mass flow should be avoided.

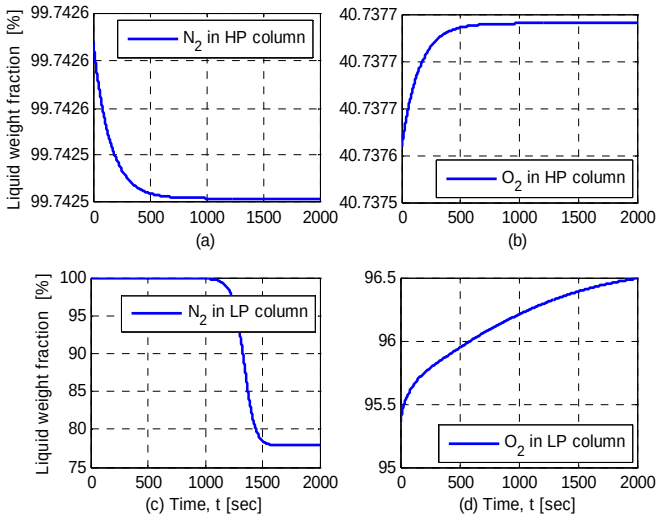


Fig.8. Dynamic responses of liquid weight fractions to a step change of product nitrogen mass flow.

### D. A step change of product oxygen mass flow

Fig.9 demonstrates the dynamic responses of liquid nitrogen and oxygen weight fractions to an increase of product oxygen mass flow from 16.4 kg/s to 20 kg/s. Similar to Figure.8, the HP column is minor impacted. Nitrogen weight fraction in LP column increases only a little while oxygen weight fraction decreased dramatically, as showed by plots (c) and (d). That is because with product oxygen mass flow increases, vapor flow and nitrogen product in LP column decrease as a result, which makes nitrogen component in the liquid flow can't be sufficiently vaporized as before, and more of it stays in the product oxygen flow.

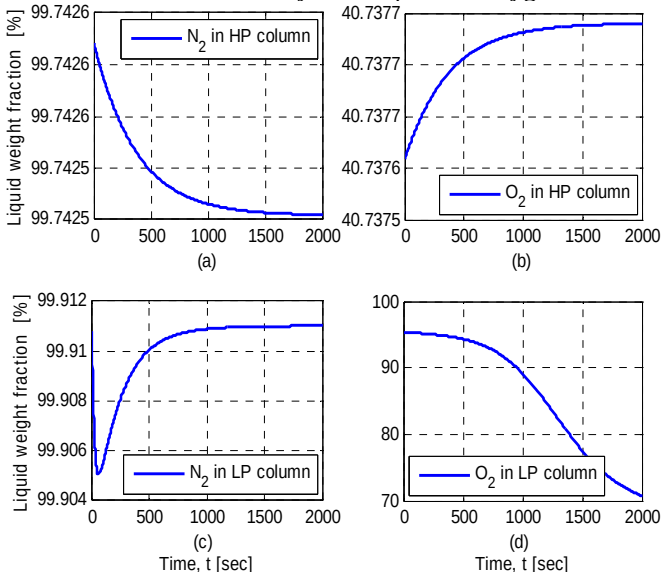


Fig.9. Dynamic responses of liquid weight fractions to a step change of oxygen product mass flow.

## V. Control Study for the Column

From simulation results given in section 4, it is seen that the process variables showed a large amount of interactions due to mutual interactions between both columns and continuous material and energy transfer among the stages. As

a result, effective control strategies should be introduced in the unit for the column to operate efficiently [19].

In this study, constrained multivariable model predictive control for the ASU has been developed as illustrated in Fig.10, and the control system is tested against a limit number of experiments. The present work is mainly concerned with the purity control for the product oxygen and nitrogen. The objective of the control system is to force the product purities to follow their set-points while the manipulated variables not changing too much or fast. Liquid levels in both columns are not included in the present study, since conventional PID controller can do a good job in level control [7].

Because product composition can be measured directly in ASU currently, the compositions are chosen as output variables in this work [20]. To design the controller for the column, the following variables are defined for the control study (see also Fig.10): the controlled variables are purities of product oxygen ($y_1$), low purity nitrogen ($y_2$) and high purity nitrogen ($y_3$), and the manipulated variables are the expand air flow ($u_1$), liquid nitrogen flow to LP column ($u_2$) and main feed air flow to HP column ($u_3$).

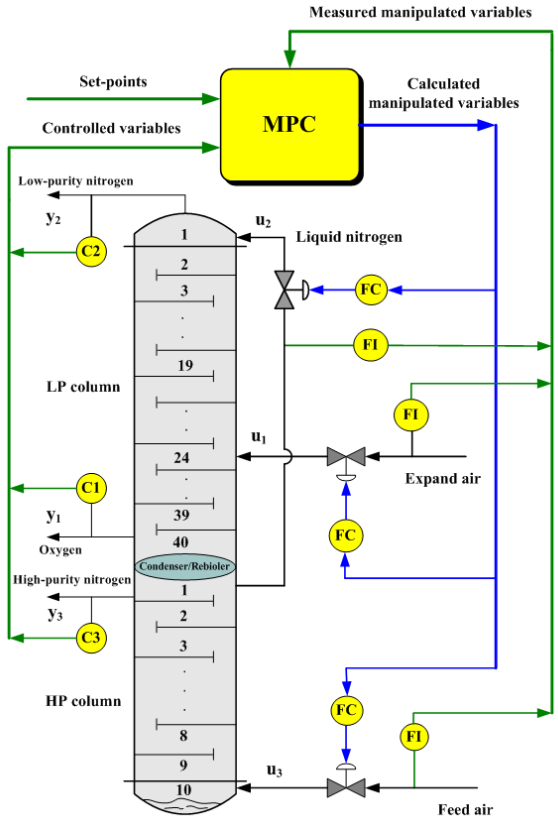


Fig.10. Multiple model predictive control structure for the column.

As for the model predictive control, the quadratic cost function is defined as a sum of quadratic future errors between the reference trajectory and predicted plant output and plant input increments, and is formulated as:

$$J_k = \sum_{j=1}^{P} Q(j)\left[\tilde{y}_P(t+j) - w_p(t+j)\right]^2 + \sum_{j=1}^{M} R(j)\Delta u^2(t+j-1) \quad (16)$$

where $\tilde{y}_P(t+j)$ denotes the vector of predicted controlled variable values, $w_p(t+j)$ the vector of reference signals, $\Delta u$ the vector of manipulated variable increments, P the predictive horizon, M the control horizon, Q the error weighting matrix, R the control weighting matrix. And in this multiple-input, multiple-output (MIMO) system, each manipulated variable influences all the outputs. And the controller parameters such as prediction and control horizon should be carefully chosen by compromise [21]. Controller parameters included in this study are: the prediction horizon P=200; control horizon M=10; output weighting Q= [1 1 1]; and input weighting R= [0.1 0.1 0.1]. At time k, the work of the multivariable MPC controller is to calculate an optimal control sequence $\Delta u = [\Delta u_1\ \Delta u_2\ \Delta u_3\ \cdots \Delta u_M]$ over the control horizon M to minimize the quadratic cost function $J_k$.

The constraints on control inputs here are as following:

$$\begin{aligned} 0 \le u_1 \le 13 \\ 26 \le u_2 \le 36 \\ 62 \le u_3 \le 82 \end{aligned} \quad (17)$$

$$\begin{aligned} -2 \le \Delta u_1 \le 2 \\ -2 \le \Delta u_2 \le 2 \\ -2 \le \Delta u_3 \le 2 \end{aligned} \quad (18)$$

The following case studies were carried out to demonstrate the performance of the MPC controller. Step changes of product oxygen, low-purity nitrogen and high-purity nitrogen purity set-points are carried out separately from t=100 to t=1000, and the objective of the control system is to keep the purity close to their set-points. And the closed-loop control results are illustrated in Fig.11, Fig.12, Fig.13 and Fig.14. In the figures plot (a) shows the responses of controlled variables and plot (b) shows the MPC controller performance.

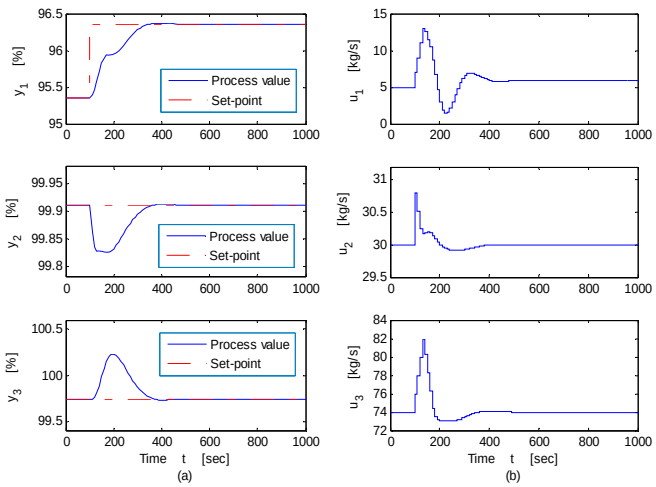


Fig.11. Closed-loop dynamic responses to a step increase of product oxygen purity set-point.

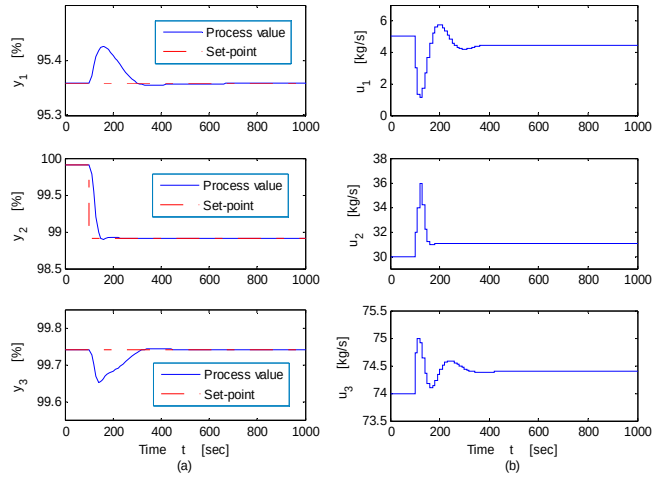


Fig.12. Closed-loop dynamic responses to a step decrease of low-purity nitrogen purity set-point

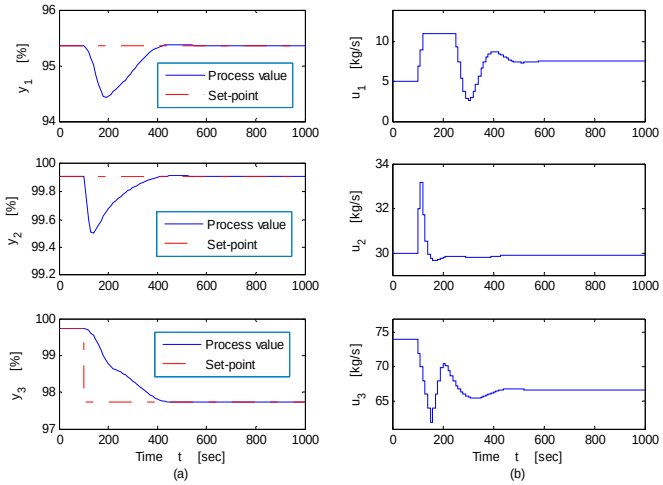


Fig.13. Closed-loop dynamic responses to a step decrease of high-purity nitrogen purity set-point.

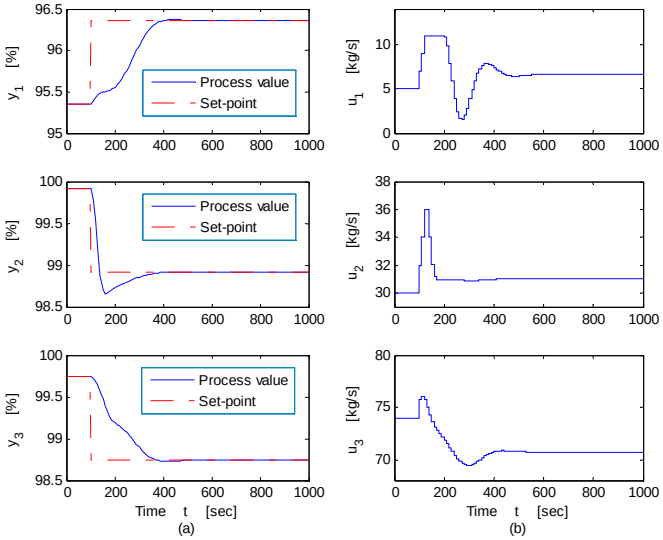


Fig.14. Closed-loop dynamic responses to step decreases of both oxygen and nitrogen purity set-points.

As observed from these figures, the proposed multivariable MPC control system shows good trajectory tracking capability and could stabilize the process within about 300 seconds, and the manipulated values and their increments are kept within certain ranges.

## VI. Conclusion

In this paper, a first–principles dynamic model of the double columns with condenser-reboiler has been developed and its dynamic responses have been studied and analyzed. Constrained MPC approach for product purity control is presented as well, and several simulation studies are carried out to test the feasibility of the control structure, and it is demonstrated that the MPC controller can do a good job.

Dynamic behaviors of ASU influence the characteristics of IGCC plant significantly, effective coordinated control strategy between ASU and the gas turbine should be our next research direction in the near future. It is expected to satisfy the product demands during normal and load-following conditions and potentially to improve the overall IGCC plant efficiency.

## Acknowledgment

The authors would like to thank Dr. Richard Hanke-Rauschenbach for his valuable assistance in the development of the ASU modeling.

## References

[1] Christou C, Hadjipaschalis I, Poullikkas A, “Assessment of integrated gasification combined cycle technology competitiveness,” Renewable Sustainable Energy Rev, doi:10.1016/j.rser, June, 2007.
[2] Beate Seliger, Richard Hanke-Rauschenbach, Frank Hannemann, Kai Sundmacher, “Modeling and dynamics of an air separation rectification column as part of an IGCC power plant,” Separation and Purification Technology , vol. 49, pp. 136-148, 2006.
[3] Hengwei Liu, Weidou Ni, Zheng Li, Linwei Ma, “Strategic thinking on IGCC development in China,” Energy Policy, vol. 36, pp. 1-11, 2008.
[4] Lifeng Zhao, Kelly Sims Gallagher, “Research, development, demonstration, and early deployment policies for advanced-coal technology in China,” Energy Policy, vol. 35, pp. 6467-6477, 2007.
[5] A.R. Smith, J. Klosek, “A review of air separation technologies and their integration with energy conversion processes,” Fuel Processing Technology, vol. 70, pp. 115-134, 2001.
[6] Gary J. Stiegel, Massood Ramezan, “Hydrogen from coal gasification: An economical pathway to a sustainable energy future,” International Journal of Coal Geology, vol. 65. pp. 173-190, 2006.
[7] B. Roffel, B.H.L. Betlem, J.A.F. de Ruijter, “First principles dynamic modeling and multivariable control of a cryogenic distillation process,” Computers and Chemical Engineering, vol. 24, pp. 111-123, 2000.
[8] Yu Zhu, Xinggao Liu, Zhiyong Zhou, “Optimization of cryogenic air separation distillation columns,” Proceedings of the 6th World Congress on Intelligent Control and Automation, Dalian, China, June 21-23, 2006.
[9] Richard Hanke, Frank Hannemann, Kai Sundmacher, “Dynamic simulation of a low-temperature rectification column as part of an IGCC power plant,” Chem. Eng. Technol, pp. 1126-1130, Nov. 2003.
[10] Peter Schoen, “Dynamic modeling and control of integrated coal gasification combined cycle units,” PhD paper, Delft: Delft University of Technology, Faculty of Mechanical Engineering and Marine Technology, Sep. 1993.
[11] Fabrizio Bezzo, Massimiliano Barolo, “Understanding the dynamic behavior of middle-vessel continuous distillation columns,” Chemical Engineering Science, vol. 60, pp. 553-563, 2005.
[12] Kejin Huang, Masaru Nakaiwa, Atsushi Tsutsumi, “Towards further internal heat integration in design of reactive distillation columns-Part II,” Chemical Engineering Science, vol. 61, pp. 5377-5392, 2006.
[13] F. Gross, E. Baumann, A. Geser, D.W.T. Rippin and L. Lang, Modeling, simulation and controllability analysis of an industrial heat-integrated distillation process. Computers Chem. Engng, vol. 22, No.1-2, pp. 223-237, 1998.
[14] Yulin Shao, Dan Golomb, “Power plants with CO2 capture using integrated air separation and flue gas recycling,” Energy Convers, vol.37, pp. 903-908, 1996.
[15] J.O. Trierweiler, S. Engell, “A case study for control structure selection: air separation plant,” Journal of Process Control, vol. 10, pp. 237-243, 2000.
[16] S. Skogestad, “Dynamic and control of distillation columns: A tutorial introduction,” Institution of Chemical Engineers, pp. 0263-8762, 1997.
[17] Myungwan Han, “Nonlinear model based control of two-product reactive distillation column,” SICE-ICASE International Joint Conference in Bexco, Busan, Korea, Oct 18-21, 2006.
[18] K. Y. Chang K. Y, William L. Luyben, “Design and control of coupled reactor/column systems-part 1: A binary coupled reactor/rectifier system,” Computers Chem. Engng, vol. 21, No.1, pp. 25-46, 1997.
[19] S. Karacan, H. Hapoglu, M. Alpbaz, Application of optimal adaptive generalized predictive control to a packed distillation column, Chemical Engineering Journal 84 (2001) 389–396.
[20] Rui Huang, Victor M. Zavala, Lorenz T. Biegler, Advanced step nonlinear model predictive control for air separation units, J. Process Contr. (2008), doi:10.1016/j.jprocont.2008.07.006.
[21] U. Volk, D.-W. Kniese, R. Hahn, R. Haber, U. Schmitz, Optimized multivariable predictive control of an industrial distillation column considering hard and soft constraints, Control Engineering Practice 13 (2005) 913 – 927.